SHORT-WAVELENGTH, SINGLE-PASS FREE-ELECTRON LASERS

J. Rossbach, DESY, 22603 Hamburg, Germany
for the TESLA FEL Group

Abstract

Impressive progress has been achieved during the past three years in demonstration of high power gain at single-pass free-electron lasers operating in the wavelength range from the infrared down to 80 nanometers. Several devices have even achieved laser saturation at gain levels exceeding one million, in agreement with theoretical expectations.

The paper summarizes some accelerator physics issues of such installations and reports mainly on results from the VUV FEL at the TESLA Test Facility (TTF FEL), including photon statistics and photon pulse length issues. Operation conditions of first user experiments at TTF FEL are discussed making use of its unrivaled peak brilliance exceeding state-of-the-art storage rings by a million times.

1 INTRODUCTION

Over the past 30 years, the synchrotron radiation has been developed into a most powerful research tool with applications in many different fields of science ranging from physics, chemistry and biology to material sciences, geophysics and medical diagnostics. Rapid progress was driven by improvements in the technology of electron storage rings and of periodic arrays of magnets called undulators thus providing increasingly brilliant sources of synchrotron radiation. The radiation generated in these devices is based on spontaneous radiation of many electrons uncorrelated in space and time. As a consequence, the radiation power scales linearly with the number N_e of electrons, and the radiation exhibits only limited coherence in space and time.

In order to increase the power and the coherence of the radiation one has to force the electrons to emit coherently by compressing them into a length small compared to the wavelength of the radiation. Passing such a "point-like" bunch of relativistic energy electrons through an undulator would cause a dramatic boost of the radiation power $P_{rad} \sim N_e^2$ with N_e the number of electrons in the bunch. Such a tight compression on an entire bunch is not possible for wavelengths in the nanometer regime. However, if one succeeds to arrange a large number of "point-like" bunchlets longitudinally into a periodic array, with the periodicity given by the wavelength of radiation, one obtains indeed coherent radiation of these bunchlets with the additional advantage of compressing all the radiation into a narrow forward cone. The principle of the Free-Electron Laser (FEL) [1] is based on this idea.

In an FEL, the density of an electrons bunch is modulated with the periodicity of the radiation wavelength λ_{ph} by a resonant process taking place in the combined presence of the periodic transverse magnetic field of an undulator and the electromagnetic radiation generated in this same magnet. The wavelength λ_{ph} of the first harmonic of the FEL radiation is related to the period length λ_u of a planar undulator by

$$\lambda_{ph} = \frac{\lambda_u}{2\gamma^2}\left(1+\frac{K^2}{2}\right) \quad , \qquad (1)$$

where $\gamma=E/(m_ec^2)$ is the relativistic factor of the electrons, and $K=eB_u\lambda_u/2\pi m_ec$ is the "undulator parameter" with B_u being the peak magnetic field in the undulator. Eq. (1) exhibits two main advantages of the free-electron laser: the free tunability of the wavelength by changing E or B_u and the possibility of achieving very short wavelengths by using ultra-relativistic electrons.

For most FELs presently in operation [2], the electron beam quality and the undulator length result in a gain in radiation power of up to a few 100% per undulator passage, making it necessary to use an optical cavity and a synchronized multi-bunch electron beam to build up high brightness upon several round-trips of the radiation in the cavity.

If one aims at very short wavelengths, where good mirrors are unavailable, high-gain FEL amplification [4,5] up to laser saturation is required within a single passage of the electron beam. This requires extreme parameters of the electron beam and a long undulator. In this mode, the radiation power P(z) is expected to grow exponentially with the distance z along the undulator.

In order to become independent of the availability of a seed laser providing the input power at the desired wavelength, the spontaneous undulator radiation from the first part of the undulator can be used as an input signal to the amplification process. Since a decade, FELs based on this Self-Amplified-Spontaneous Emission (SASE) principle [5] are considered the most promising candidates for extremely brilliant, coherent light sources with wavelengths down to the Angström regime [6-8].

2 STATE OF THE ART SASE OPERATION

The rapid progress in the construction and understanding of short-wavelength SASE FELs is best illustrated by the successful demonstration of FEL saturation for submicrometer wavelengths at three different laboratories, and the excellent agreement between observation and theory in all three cases.

2.1 Demonstration of FEL saturation

Figure 1 shows the exponential growth by more than 7 orders of magnitude in radiation power observed at the VISA FEL. The onset of laser saturation is clearly seen close to the exit of the undulator and takes place at the expected power level [9].

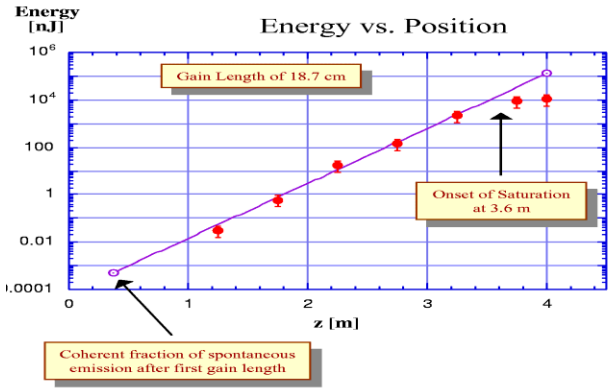

Figure 1: Demonstration of exponential growth of radiation energy at the VISA FEL at 845 nm radiation wavelength [9].

As illustrated in Figure 2, the LEUTL experiment at Argonne Natl. Lab., USA, was successful in demonstrating FEL saturation at 530 nm, 385 nm [10], and 265 nm [11] wavelength. Since the power gain length (i.e. the e-folding length of radiation energy during the exponential growth) has the tendency to increase with decreasing wavelength, the LEUTL undulator has a total length of 25 m (the effective length is approx. 22 m because of some drift spaces between undulator segments equipped with electron focusing and radiation diagnostics).

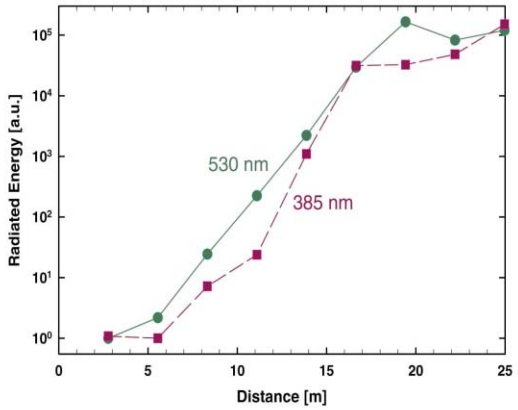

Figure 2: LEUTL FEL gain at 530 nm and 385 nm wavelength [10]. Saturation was also achieved at 265 nm radiation wavelength [11].

FEL action at the shortest wavelength achieved so far has been demonstrated at TTF FEL at DESY, Germany. SASE FEL gain was observed up to saturation level in the range from 80 nm to 120 nm, see Figure 3 [12]. Similar to the VISA and LEUTL results, saturation sets in at the predicted power level. Details of the TTF FEL technical layout can be found in Refs. [13,14].

While VISA and LEUTL have been proof-of-principle experiments on the SASE principle, without any ambition to deliver radiation to scientific users, the TTF FEL result plays a particular role as it demonstrates the SASE FEL principle for the first time in a wavelength regime where it is clearly superior to classical lasers and to optical cavity FELs.

The peak brilliance of the TTF FEL photon beam exceeds that of any other source at this wavelength by several orders of magnitude. In particular, in comparison to the performance of state-of-the-art synchrotron radiation storage rings operating at this wavelength, the peak brilliance is larger by 8 orders of magnitude. The peak power is at the 1 GW level, corresponding to 2×10^{13} photons per pulse of 50 fs length (FWHM).

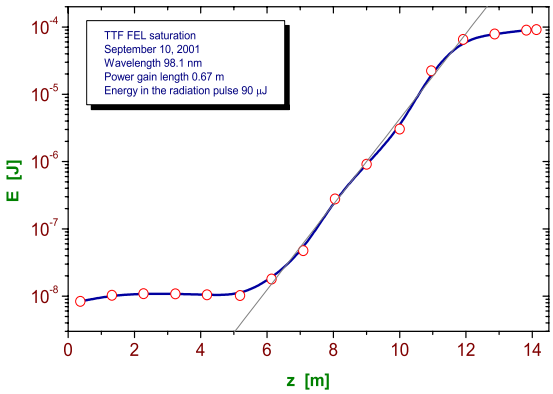

Figure 3: Demonstration of SASE exponential growth and saturation at the TTF FEL, DESY, Hamburg [12]. The undulator is approx. 15 m long.

As a consequence of this extraordinary photon beam quality, first scientific pilot experiments were performed already a few weeks after FEL saturation was demonstrated. The operation statistics during one week of user operation is shown in Figure 4. The availability for users was some 65 % during this early week of "routine" operation.

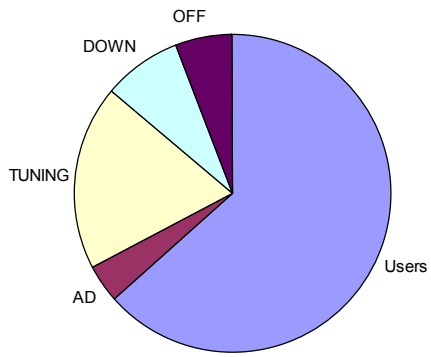

Figure 4: Reliability of TTF FEL during one week of operation for scientific users. The statistics was taken only short time after saturation was demonstrated for the first time.

2.2 Properties of SASE FEL radiation

In addition to the energy in each FEL pulse as discussed above, there are three more properties of the FEL radiation relevant to users:

- Transverse coherence

- Longitudinal coherence and/or pulse duration
- Fluctuation behaviour

According to FEL theory, one expects almost perfect transverse coherence close to saturation. Figure 5 shows two diffraction patterns of the TTF FEL radiation measured with a gated CCD camera viewing a Ce:YAG screen in a distance of 3 m behind a double slit and two crossed slits, respectively [14]. The slits are located 12m behind the exit of the undulator. The remarkable high fringe visibility is a proof of the high degree of transverse coherence. This interpretation has been corroborated by measurement of the opening angle of the radiation [12].

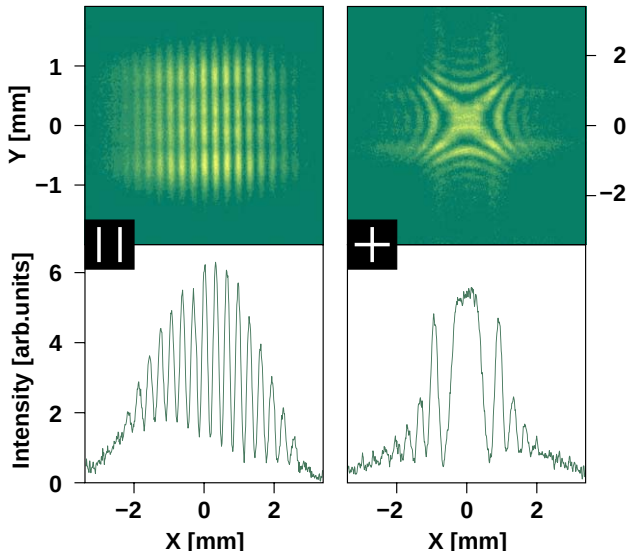

Figure 5: Diffraction pattern of two different slit arrangements (see pictographs) illustrating the transverse coherence of the radiation at TTF FEL [14]; left: double slit, each slit 2 mm (vert.) × 200 μm (horiz.); right: crossed slits, each slit 4 mm × 100 μm. The lower part of both images depicts a horizontal cut through the centre of the respective diffraction pattern. Due to the size of the slits it is guaranteed that almost the entire FEL radiation takes part in the interference, thus indication that the degree of transverse coherence is very high.

Measurements of the spectral distribution are presented in Figure 6 [14]. Single-shot spectra were taken with a monochromator of 0.2 nm resolution equipped with an intensified CCD camera [15]. They show an ensemble of a few peaks which reflect the number M of longitudinal modes in the radiation pulse [16] as it is expected for SASE FEL radiation starting from shot noise.

The pulse duration is a very important parameter but not presently accessible to direct measurement in the time domain. The approximate pulse length τ_{rad} can however be calculated from the FWHM spectral width $\Delta\omega$ of each peak in the single shot spectrum by $\tau_{rad} \approx 2\pi/\Delta\omega$. For the spectrum shown in the upper part of Figure 6 this results in $\tau_{rad} \approx 40$ fs. The lower plot in Figure 6 was taken with a bunch compressor setting for longer pulses. Consequently, the number of modes is larger (in average, M=6) and the spectral width $\Delta\omega$ of each spike is smaller, resulting in $\tau_{rad} \approx 100$ fs.

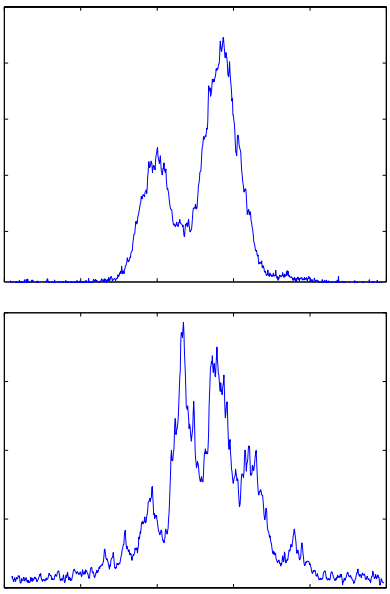

Figure 6: Spectra from short (top) and long (bottom) FEL pulses. It is seen that the number of longitudinal optical modes depends on electron bunch length which can be varied by tuning the bunch compressor settings. For short pulses (duration $\tau_{rad} \approx 40$ fs) there are, in average, 2.6 modes, while in the long bunch pulse setting ($\tau_{rad} \approx 100$ fs, bottom) there are 6 modes in average.

2.3 Fluctuations of FEL pulse energy

Since SASE FEL radiation results from amplification of spontaneous undulator radiation, the pulse energy is subject to the same statistics. Thus, the spectra shown in Figure 6 will change from pulse to pulse, but they will always stay within the bandwidth of FEL amplification, and the average number of modes will remain unchanged for each bunch compressor setting. In addition to fluctuations of the single pulse spectra, there are also fluctuations of the pulse-to-pulse intensity. In the regime of exponential growth, the radiation pulse energy is expected to fluctuate according to a gamma distribution p(E) [16]:

$$p(E) = \frac{M^M}{\Gamma(M)} \left(\frac{E}{\langle E \rangle} \right)^{M-1} \frac{1}{\langle E \rangle} \exp\left(-M \frac{E}{\langle E \rangle} \right) \qquad (2)$$

where <E> is the mean energy, Γ(M) is the gamma function with argument M, and $M^{-1} = \langle (E - \langle E \rangle)^2 \rangle / \langle E \rangle^2$ is the normalized variance of E. M corresponds to the number of optical modes, which gives an intimate relationship between the number of modes (spikes) derived from single pulse spectra and the fluctuation (and distribution function) of pulse energy. Figure 7 illustrates

the pulse--to-pulse fluctuation of SASE pulse energy for different settings of the electron bunch length at TTF FEL at DESY [14]. The left and middle settings correspond to the settings used for Figure 6. If one extracts the mode numbers 6 and 2.6, respectively, from the number of spikes in Figure 6, then there in no more free parameter in the determination of the probability distribution of pulse energies. As seen from Figure 7, the agreement between measurements and the expected distribution calculated from Eq. (2) (solid curves in the histograms) is very good.

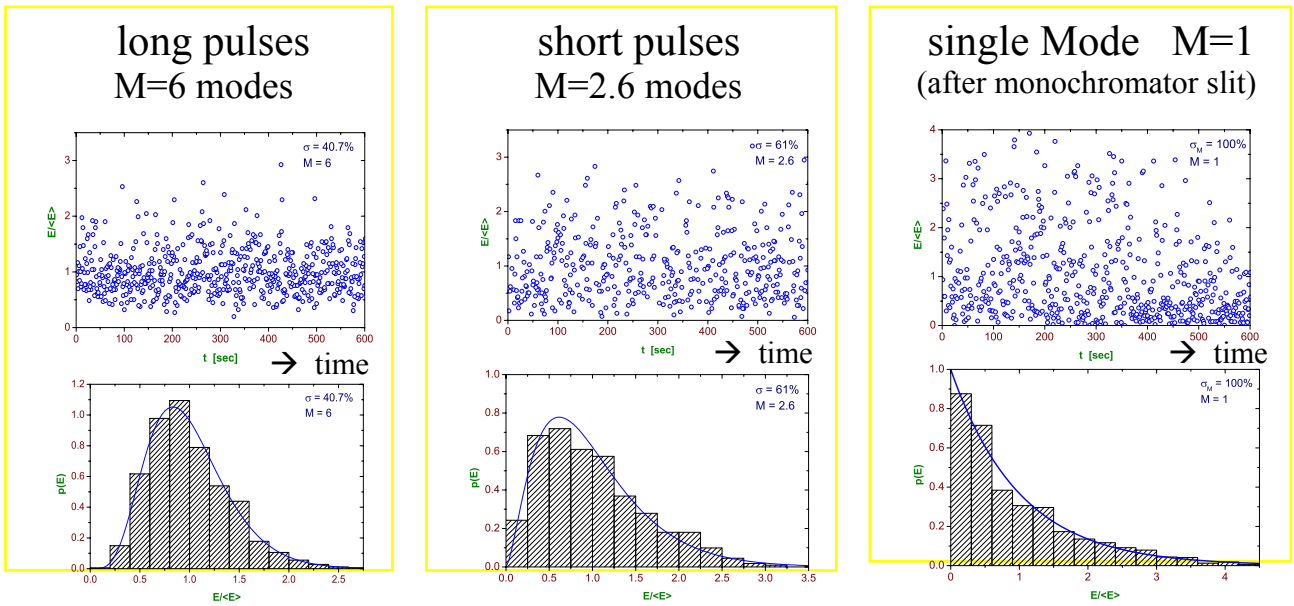

Figure 7: Pulse-to-pulse fluctuation of SASE pulse energy for different settings of electron bunch length at TTF FEL at DESY. Upper row: measured single pulse energy versus time; lower row: histogram of probability distribution extracted from the measurement. The SASE pulses are observed at high gain, but still in the exponential regime, not yet in saturation. The plots on the right hand side illustrate the case of a single mode which can be realized, for instance, by accepting only the radiation that has passed a monochromator slit.

Table 1: SASE FEL facilities

Name	**Location**	**Min. wavelength**	**Year of first FEL operation**	**Reference**
a) Projects under progress				
TTF2 FEL	DESY	6 nm	2004	[17]
SCSS	Spring8	3.6 nm	2005	[18]
LCLS	SLAC	0.15 nm	2008	[19]
b) proposed projects				
SPARX/FERMI	Italy	1.5 nm	2005	[20]
BESSY III	Berlin	1 nm	ca. 2007	[21]
TESLA XFEL	DESY	0.085 nm	2011	[8]

3 OVERVIEW OF SASE FEL PROJECTS

Encouraged by the progress described above, a number of SASE FEL facilities are worldwide either under progress or being proposed. They are summarized in Table 1.

Figure 8 shows the linac tunnel (covered with sand for shielding) and the experimental hall for the TTF2 FEL at DESY.

For the TESLA X-ray FEL laboratory proposed as part of the TESLA project, it was originally planned to share the first part of the superconducting electron linac with the linear collider in an alternating rf pulse mode [8], mainly for cost saving reasons. Following a recommendation by the German Wissenschaftrat, this design has now been modified towards a solution where the XFEL has its own linac thus avoiding unwanted coupling between collider and XFEL operation, and to allow for more flexibility in XFEL beam parameter space. This modified layout is schematically shown in Figure 9. It keeps all the other advantages of a joint project like savings in hardware, personnel and land, potential synergetic effects from various research communities on the same site, and it keeps the option of sharing part of the collider linac in a later stage.

Figure 8: Photograph of TTF2 at DESY. The hall in the background is housing TTF1, and in the foreground the experimental hall for scientific users of TTF2 FEL is seen.

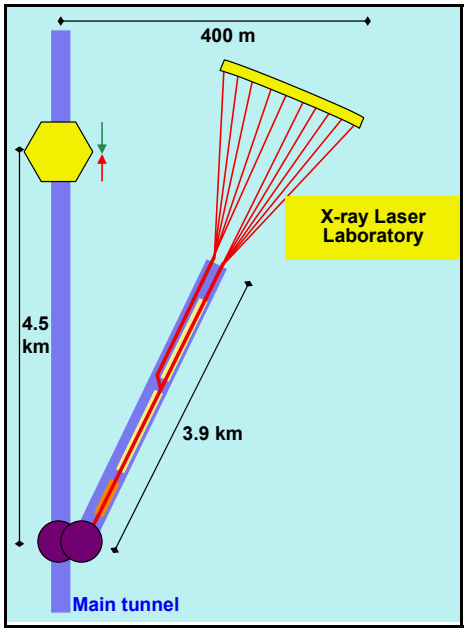

Figure 9: Schematic layout of the X-ray laser laboraratory with its own linac, proposed as part of the TESLA project.

4 ACKNOWLEDGEMENT

The author acknowledges valuable information and material provided by other FEL groups, in particular by the VISA, the LEUTL and the LCLS group.

5 REFERENCES

[1] J.M.J. Madey, J Appl. Phys. **42**, 1906 (1971)
[2] W.B. Colson, Nucl. Instr. Meth**. A 475**, 397 (2000)
[3] K.J. Kim, Phys. Rev. Lett. **57,** 1871 (1986)
[4] E.L. Saldin, E.A. Schneidmiller, M.V. Yurkov, *The Physics of Free-Electron Lasers* (Springer, 1999) and references therein
[5] A.M. Kondratenko, E.L. Saldin, Part. Accelerators **10**, 207 (1980)
[6] H. Winick et al., Proc. PAC, Washington and SLAC-PUB-6185 (1993)
[7] R. Brinkmann, et al., Nucl. Instr. Meth. **A 393**, 86 (1997)
[8] TESLA Technical Design Report, edited by F. Richard et al., DESY 2001-011 and http://tesla.desy.de
[9] A. Murokh, et al., Proc. 2001 Part Acc. Conf. Chicago (2001)
[10] S. Milton et al, Science **292**, 2037 (2001)
[11] S. Milton, private communication
[12] V. Ayvazyan et al., Phys. Rev. Lett. **88**, No.10 (2002)
[13] H. Weise, this conference
[14] V. Ayvazyan, et al., Eur. Phys. J. D, 149 (2002)
[15] R. Treusch, et al., Nucl. Instr. Meth. **A445**, 456 (2000)
[16] E.L.Saldin, E.A. Schneidmiller, M.V. Yurkov, Opt. Commun. **148**, 383 (1998)
[17] M. Körfer, Nucl. Instr. Meth. **A483**, 34 (2002)
[18] T. Shintake, et al., this conference
[19] J. Galayda, this conference
[20] L. Serafini, this conference
[21] M. Abo-Bakr, et al, Nucl. Instr. Meth. **A483**, 470 (2002)